Since January 2020 Elsevier has created a COVID-19 resource centre with free information in English and Mandarin on the novel coronavirus COVID-19. The COVID-19 resource centre is hosted on Elsevier Connect, the company's public news and information website.

Virology 556 (2021) 96–100

Contents lists available at ScienceDirect

Virology

journal homepage: www.elsevier.com/locate/virology

The G614 pandemic SARS-CoV-2 variant is not more pathogenic than the original D614 form in adult Syrian hamsters

Charles B. Stauft, Christopher Z. Lien, Prabhuanand Selvaraj, Shufeng Liu, Tony T. Wang *

Laboratory of Vector-Borne Diseases, Division of Viral Products, Office of Vaccine Research and Review, Food and Drug Administration, White Oak, MD, USA

ARTICLE INFO

Keywords:
SARS-CoV-2
COVID-19
Severe acute respiratory syndrome
Coronavirus
Hamster model
Syrian hamsters
Spike protein

ABSTRACT

Dynamic tracking of variant frequencies among viruses circulating in the global pandemic has revealed the emergence and dominance of a D614G mutation in the SARS-CoV-2 spike protein. To address whether pandemic SARS-CoV-2 G614 variant has evolved to become more pathogenic, we infected adult hamsters (>10 months old) with two natural SARS-CoV-2 variants carrying either D614 or G614 spike protein to mimic infection of the adult/elderly human population. Hamsters infected by the two variants exhibited comparable viral loads and pathology in lung tissues as well as similar amounts of virus shed in nasal washes. Altogether, our study does not find that naturally circulating D614 and G614 SARS-CoV-2 variants differ significantly in pathogenicity in hamsters.

1. Introduction

Severe Acute Respiratory Syndrome Associated Virus 2 (SARS-CoV-2) is a *betacoronavirus* with many similarities to SARS-CoV-1. Like other coronaviruses, the SARS-CoV-2 virion is studded with a corona of spike proteins that are essential for host receptor binding. In a landmark paper published in Cell, Korber et al. described the emergence and dominance of a D614G mutation in the SARS-CoV-2 spike protein during the ongoing pandemic (Korber et al., 2020). Of concern, the D614G mutation was associated with elevated viral loads observed in infected patients and enhanced replication of pseudotyped virions (Korber et al., 2020; Yurkovetskiy et al., 2020). However, there was no significant association between the D614G mutation and disease severity (Korber et al., 2020). A very recent preprint reported that an engineered D614G mutation significantly enhances SARS-CoV-2 replication on human lung epithelial cells and primary human airway tissues (Plante et al., 2020), and there is as of yet limited literature on the effects of mutations on SARS-CoV-2 pathogenesis. Because of the genomic proof-reading capacity of coronaviruses (Maier et al., 2015), the observation of a new genotype overtaking the initial strain warrants close attention.

The question of whether the D614G mutation increases virulence or pathogenicity of SARS-CoV-2 in humans remains unanswered. We employed an adult hamster pathogenesis model to address whether SARS-CoV-2 evolution during the current pandemic resulted in increased pathogenesis. Syrian hamsters (*Mesocricetus auratus*) can live to be 18-24 months old and reach sexual maturity after ~12-13 weeks of age. However, studies commonly employ 5-10-week-old hamsters which are more logistically viable but immature (Brocato et al., 2020; Chan et al., 2020a, 2020b; Kreye et al., 2020). As advanced age strongly correlates with severe disease in COVID-19 patients (Hu et al., 2020), aged hamsters support higher levels of viral replication than younger hamsters and even developed possibly lethal pneumonia after infection (Liu, 2020; Selvaraj, 2021).

2. Materials and methods

2.1. Virus and cell culture

SARS-CoV-2/human/USA/USA-WA1/2020 (GenBank: MT2466 67.1) and SARS-CoV-2/human/USA/NY-PV08410/2020 were propagated in Vero E6 cells to generate working virus stocks with infectious titers of $4.7x10^6$ pfu/ml and $1.8x10^7$ pfu/ml, respectively, and sequenced to confirm genotypes.

Vero E6 cells (ATCC, Manassas VA) were grown in Dulbecco's Modified Eagle's Medium (Corning) supplemented with 10% fetal bovine serum (FBS) and penicillin/streptomycin. Human embryonic kidney (HEK-293T) cells expressing Lenti-X were also grown in DMEM supplemented with 10% FBS and penicillin/streptomycin.

* Corresponding author.
E-mail address: Tony.Wang@hhs.fda.gov (T.T. Wang).

https://doi.org/10.1016/j.virol.2021.01.005
Received 21 October 2020; Received in revised form 21 December 2020; Accepted 11 January 2021
Available online 25 January 2021

2.2. Sequencing of viral stocks

To prepare sequencing libraries, 20 μl RNA was extracted from 140 μl virus stock and RNA quality was assessed by Agilent 2100 Bioanalyzer (Agilent Technologies, Santa Clara, CA, USA) to confirm that the RNA integration numbers (RIN) were all greater than 9. Library preparation followed the "Illumina section 2 c) Illumina shotgun metagenomics" (https://github.com/CDCgov/SARS-CoV-2_Sequencing) protocol with minor changes (Supplementary methods).

2.3. SARS-CoV-2 pseudovirus production and neutralization assay

Human codon-optimized cDNA encoding D614 SARS-CoV-2 S glycoprotein from the Wuhan-Hu-1 isolate (NC_045512) was synthesized by GenScript and cloned into eukaryotic cell expression vector pcDNA 3.1 between the BamHI and XhoI sites. Pseudovirions were produced by co-transfection of Lenti-X 293T cells with psPAX2, pTRIP-luc, and SARS-CoV-2 S expressing plasmid using Lipofectamine 3000. The supernatants were harvested at 48 h and 72 h post-transfection and filtered through 0.45-mm membranes prior to use.

For the neutralization assay, 50 μL of SARS-CoV-2 S pseudovirions were pre-incubated with an equal volume of medium containing serum at varying dilutions at room temperature for 1 h, then virus-antibody mixtures were added to Vero E6 cells in a 96-well plate. After a 3 h incubation, the inoculum was replaced with fresh medium. Cells were lysed 48 h later, and luciferase activity was measured using luciferin-containing substrate. Controls included cell only control, virus without any antibody control and positive control sera. The end-point titers were calculated as the last serum dilution resulting in at least 50% SARS-CoV-2 neutralization.

2.4. Hamster challenge experiments

All experiments were performed within the biosafety level 3 (BSL-3) suite on the White Oak campus of the U.S. Food and Drug Administration (FDA). Aged male and female outbred Syrian hamsters were purchased from Envigo at 4-5 weeks old and held at the FDA vivarium. The animals were implanted subcutaneously with IPTT-300 transponders (BMDS), randomized, and housed 2 per cage in sealed, individually-ventilated rat cages (Allentown). Hamsters were fed irradiated 5P76 (Lab Diet) *ad lib*, housed on autoclaved aspen chip bedding with reverse osmosis-treated water provided in bottles, and all animals were acclimatized at the BSL3 facility for 4-6 days or more prior to the experiments. The study protocol details were approved by the White Oak Consolidated Animal Care and Use Committee and carried out in accordance with the PHS Policy on Humane Care & Use of Laboratory Animals.

For challenge studies, aged (10-20 months old) Syrian hamsters were anesthetized with intraperitoneal injection of 50 mg/kg ketamine + 0.15 mg/kg dexmedetomidine. Intranasal inoculation was done with 10^3 or 10^5 $TCID_{50}$ SARS-CoV-2 in 50-100 μl volume dropwise into the nostrils. Each hamster then received 3.3 mg/kg diluted atipamezole solution intraperitoneally immediately after intranasal inoculation. Hamsters were weighed and assessed daily. Nasal washes were collected by pipetting ~160 μl sterile phosphate buffered saline into one nostril when hamsters were anesthetized by 3-5% isoflurane. For tissue collection, hamsters were first euthanized by intraperitoneal injection of pentobarbital at 200 mg/kg.

2.5. RNA isolation and qRT-PCR

RNA was extracted from 50 μl nasal wash or 0.1-g tissue homogenates using QIAamp viral RNA mini kit or the RNeasy 96 kit (Qiagen) and eluted with 60 μL of water. Five μL RNA was used for each reaction in real-time RT-PCR.

Quantification of SARS-CoV-2 viral RNA (vRNA) was conducted using the SARS-CoV-2 (2019-nCoV) CDC qPCR Probe Assay (IDTDNA) using iTaq Universal Probes One-Step Kit (Bio-Rad). The standard curve was generated using 2019-nCoV_N_Positive Control (IDTDNA). The detection limit of the vRNA was determined to be 100 copies/reaction. Quantification of SARS-CoV-2 E gene subgenomic mRNA (sgmRNA) was conducted using Luna Universal Probe One-Step RT-qPCR Kit (New England Biolabs) on a Step One Plus Real-Time PCR system (Applied Biosystems). The primer and probe sequences were: SARS2EF: CGATCTCTTGTAGATCTGTTCT;PROBE:FAM-ACACTAGCCATCCTTACT GCGCTTCG- BHQ-1; SARS2ER: ATATTGCAGCAGTACGCACACA. To generate a standard curve, the cDNA of SARS-CoV-2 E gene sgmRNA was cloned into a pCR2.1-TOPO plasmid. The copy number of sgmRNA was calculated by comparing to a standard curve obtained with serial dilutions of the standard plasmid. The detection limit of the sgmRNA was determined to be 25 copies/reaction. Values below detection limits were mathematically extrapolated based on the standard curves for graphing purpose.

2.6. Histopathology analyses

Lung samples were fixed in 10% neural buffered formalin overnight and then processed for paraffin embedding. The 4-μm sections were stained with hematoxylin and eosin for histopathological examinations. Images were scanned using an Aperio ImageScope.

To detect SARS-CoV-2 genomic RNA in FFPE tissues, *in situ* hybridization (ISH) was performed using the RNAscope 2.5 HD RED kit, a single plex assay method (Advanced Cell Diagnostics; Catalog 322373) following the manual according to the manufacturer's instructions with a probe targeting SARS-CoV-2 spike genomic (positive-sense) RNA (Supplementary methods).

3. Results

To allow head-to-head comparison between real-world variants, we cultured two virus isolates USA-WA1/2020 (D614) and New York-PV08410/2020 (G614), which started circulating in the United States from February 2020 in the West and East coast, respectively. The two isolates differ by 5 amino acids including position 614 of spike protein (Table 1). The sequences of our cultures prepared from the clinical isolates were confirmed by sequencing with approximately 1,250-2,500X coverage of the viral genome.

It was previously reported that VSV and lentiviral pseudoviruses expressing the G614 SARS-CoV-2 spike protein exhibit increased infectivity *in vitro* (Korber et al., 2020; Yurkovetskiy et al., 2020; Zhang et al., 2020). Confirming these prior studies with wild-type SARS-CoV-2, we noticed that the viral stocks of G614 were up to 5 times higher than D614 in Vero E6 cells, however, the plaque size was not observed to be markedly different between the two (Fig. 1D). Although increased replication was observed in cultured cells, we tested whether a G614 SARS-CoV-2 clinical isolate would show increased replication, pathogenicity, and shedding *in vivo*. To test these hypotheses, we inoculated adult Syrian hamsters (11 months old) by the intranasal route with 1,

Table 1
Summary of differences between the D614 and G614 SARS-CoV-2 genomic sequences.

Genome Position (D614 nt)	Mutation	Amino Acid Change (protein)
241	C to T	5' UTR
1059	C to T	Thr to Ile ORF1ab aa 265
3037	C to T	none (aa924 of ORF1ab Phe)
8782	T to C	none (aa 2839 of ORF1ab Ser)
14407	C to T	Pro to Ser (aa4715 of ORF1ab)
23403	A to G	Asp to Gly (aa614 of Spike)
25563	G to T	Gln to His (aa57 of ORF3a)
28144	C to T	Ser to Leu (aa84 of ORF 8)

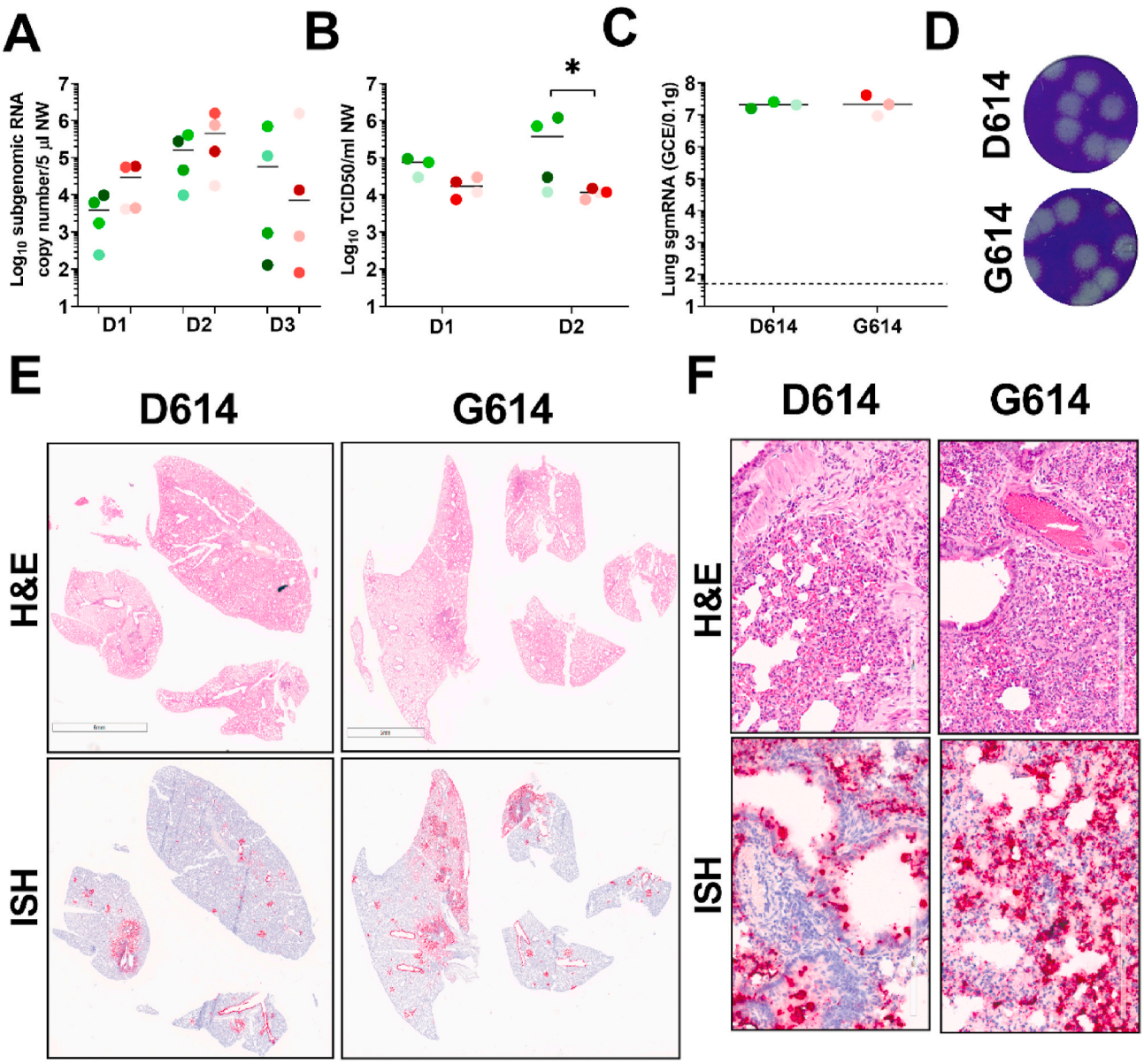

Fig. 1. Aged hamsters (>10 months old) show comparable viral loads and pathology after infection with either D614 or G614 SARS-CoV-2. Following intranasal inoculation with 10^3 $TCID_{50}$ SARS-CoV-2 D614 or G614, levels of viral replication were measured in nasal washes using either qRT-PCR (A) or $TCID_{50}$ assay (B). Viral loads in the lungs of infected hamsters were measured on day 3 post-infection using qRT-PCR with primers specific for subgenomic RNA (C). Plaque phenotypes of D614 and G614 grown in Vero E6 cells (D). On day 3 lungs were dissected from each animal and stained to examine pathology (H&E) and viral antigens (ISH) from D614 or G614 infection. Whole lung (E) and 20X slide views are shown (F). D1, D2, D3 stand for days 1, 2, or 3 post-infection. H&E stands for hematoxylin and eosin. ISH stands for *in situ* hybridization.

000 $TCID_{50}$ of D614 or G614 SARS-CoV-2 and measured viral loads post-infection in lungs and nasal washes to compare virulence (Fig. 1). Viral RNA levels in nasal washes were not found to be significantly different on days 1, 2, or 3 post-infection (Fig. 1A) while infectious viral titers ($TCID_{50}$) were slightly but significantly ($p = 0.0363$, Student's t-test) lower in the nasal washes of G614 infected hamsters (Fig. 1B). On day 3, lungs ($n = 3$) from both treatment groups were removed for titration and pathology. Replicating virus was targeted using quantification of subgenomic RNA by qRT-PCR, however, no difference was observed between D614 and G614 infected hamsters (Fig. 1C). As expected for SARS-CoV-2 infection, we observed considerable consolidation as well as the presence of viral replication in lungs harvested at day 3 post-infection with 10^3 $TCID_{50}$ of either D614 or G614 SARS-CoV-2 (Fig. 1E/1F). Overall, when comparing D614 and G614 infected lungs SARS-CoV-2 we observed no overt difference in lung pathology.

Next, adult Syrian hamsters (11 months old) were inoculated by the intranasal route with 10^5 $TCID_{50}$ of a D614 or G614 virus. On average hamsters in both groups lost up to 14% body weight in 7 days, however the amount of weight loss was comparable for both D614 and G614 over the course of two weeks (Fig. 2A). On day 12, the infected hamsters were terminally bled, and serum collected for neutralizing antibody titration (NT50). No significant different in neutralizing antibody titer against D614-derived virus was observed (Fig. 2B). Examination of the infected lungs at Day 12 post-infection revealed 40-60% consolidation (Fig. 2C and 2D) in both groups. Abundant atypical hyperplasia and hypertrophy of terminal bronchiolar epithelial cells and pneumocytes were noticed along with interstitial lymphocytic infiltrates. Nonetheless, there were no significant differences between the two groups.

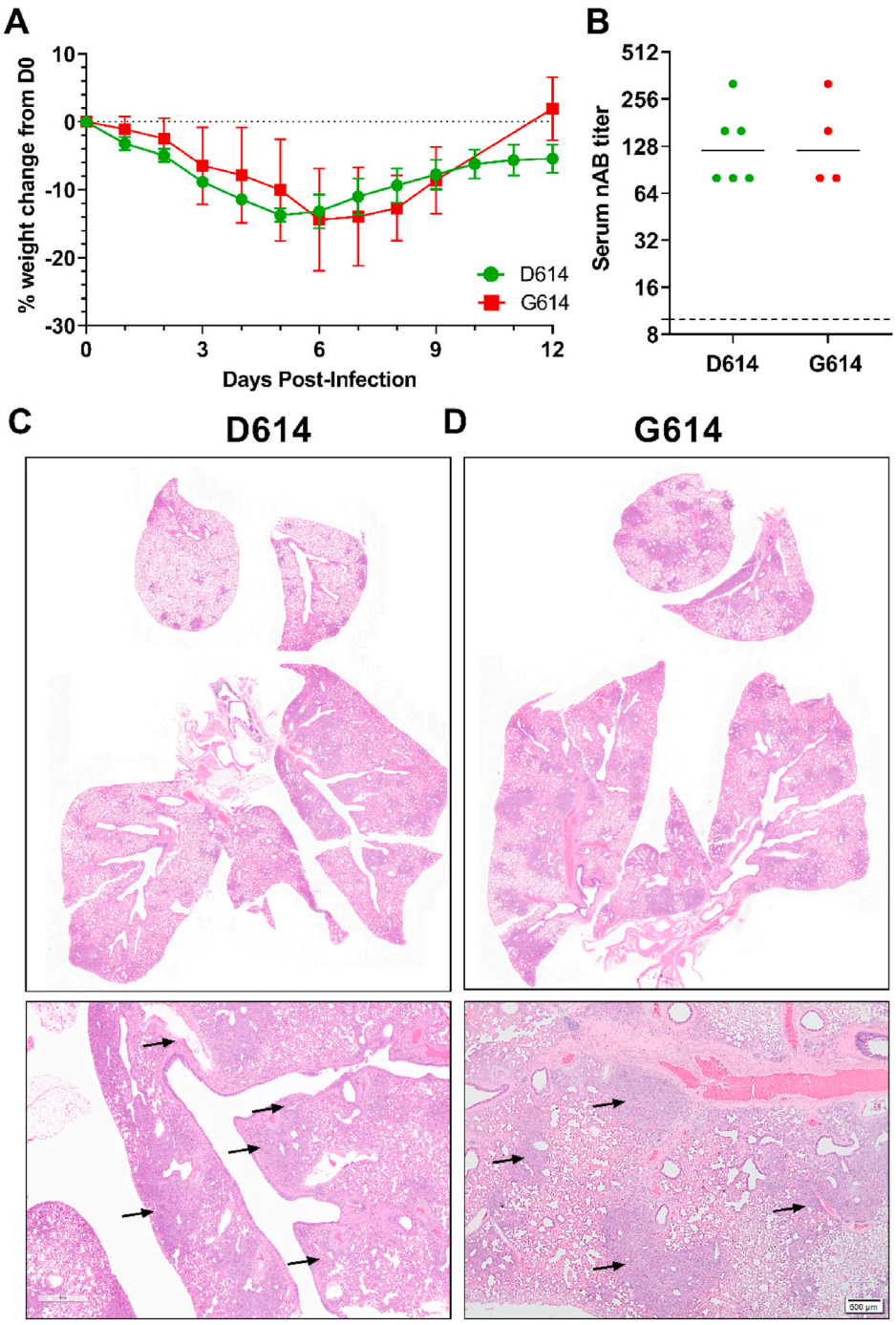

Fig. 2. Aged hamsters (>10 months old) show comparable weight loss, neutralizing antibody titers, and pathology after infection with either D614 or G614 SARS-CoV-2. Following intranasal inoculation of adult hamsters with 10^5 $TCID_{50}$ SARS-CoV-2 D614 (red circles) or G614 (green squares), morbidity (weight loss) was followed daily for 12 days post-infection (A). After 12 days post-infection, blood was collected from all animals and tested for neutralizing antibodies (B). On day 12, pathology was compared in fixed lung tissue harvested from D614 (C) and G614 (D) SARS-CoV-2 infected adult hamsters. Black arrows indicate areas with consolidation.

4. Discussion

Although multiple studies, including ours, show the G614 variant grows to a higher titer (Korber et al., 2020; Yurkovetskiy et al., 2020; Zhang et al., 2020), it is unclear whether the fixation of D614G spike mutation is the result of a founder effect as the SARS-CoV-2 pandemic spread to Europe and the Americas or a product of viral evolution in response to a new host or to some other selective pressure. Rather than use recombinant SARS-CoV-2, which would focus on the single D614G mutation, we chose two isolates from US patients that were collected at different time periods during the pandemic. A limitation to this study is that the chosen G614 variant has multiple nucleic acid changes compared to the D614 variant (Table 1), hence any potential effect conferred by the G614 may be masked by that of other amino acid changes. Indeed, a recent study showed that a recombinant G614 virus produced higher infectious titers in the nasal washes and trachea, but not lungs, than the D614 virus (Plante et al., 2020). Nonetheless, choosing real-world isolates makes our model more relevant to study the ongoing COVID-19 pandemic.

In the adult Syrian hamster model, we were unable to discern a detectable increase in pathogenicity with a G614 isolate of SARS-CoV-2 in hamsters, as has been observed clinically. Although recovery of body weight in infected hamsters was observed by day 12, continued lung pathology was still observable in lung tissues, with no marked difference between the two strains of SARS-CoV-2. Therefore, G614 may confer some growth advantage over the original D614 form but does not alter the overall pathogenicity of the virus.

5. Conclusions

In this study, adult Syrian hamsters infected by either a natural D614 or G614 SARS-CoV-2 variant did not exhibit significant differences in terms of viral loads and histopathology in the lung, arguing that naturally circulating D614 and G614 SARS-CoV-2 variants do not differ significantly in pathogenicity in hamsters.

CRediT authorship contribution statement

Charles B. Stauft: Formal analysis, Investigation, Writing - original draft, Visualization. **Christopher Z. Lien:** Investigation. **Prabhuanand Selvaraj:** Methodology, Investigation, Writing - original draft. **Shufeng Liu:** Methodology, Investigation. **Tony T. Wang:** Conceptualization, Methodology, Investigation, Writing - original draft, Visualization, Supervision, Project administration.

Declaration of competing interest

None.

Acknowledgements

Our work was funded by internal US FDA funding.

Appendix A. Supplementary data

Supplementary data to this article can be found online at https://doi.org/10.1016/j.virol.2021.01.005.

References

Brocato, R.L., et al., 2020. Disruption of adaptive immunity enhances disease in SARS-CoV-2 infected Syrian hamsters. J. Virol. https://doi.org/10.1128/JVI.01683-20.

Chan, J.F., et al., 2020a. Surgical mask partition reduces the risk of non-contact transmission in a golden Syrian hamster model for Coronavirus Disease 2019 (COVID-19). Clin. Infect. Dis. https://doi.org/10.1093/cid/ciaa644.

Chan, J.F., et al., 2020b. Simulation of the clinical and pathological manifestations of Coronavirus Disease 2019 (COVID-19) in golden Syrian hamster model: implications for disease pathogenesis and transmissibility. Clin. Infect. Dis. https://doi.org/10.1093/cid/ciaa325.

Hu, S., et al., 2020. Infectivity, susceptibility, and risk factors associated with SARS-CoV-2 transmission under intensive contact tracing in Hunan, China. medRxiv. https://doi.org/10.1101/2020.07.23.20160317.

Korber, B., et al., 2020. Tracking changes in SARS-CoV-2 spike: evidence that D614G increases infectivity of the COVID-19 virus. Cell 182, 812–827. https://doi.org/10.1016/j.cell.2020.06.043 e819.

Kreye, J., et al., 2020. A SARS-CoV-2 neutralizing antibody protects from lung pathology in a COVID-19 hamster model. bioRxiv. https://doi.org/10.1101/2020.08.15.252320.

Liu, S., et al., 2020. The PRRA insert at the S1/S2 site modulates cellular tropism of SARS-CoV-2 and ACE2 usage by the closely related Bat raTG13. bioRxiv, 2020.2007.2020.213280. https://doi.org/10.1101/2020.07.20.213280.

Maier, H.J., Bickerton, E., Britton, P., 2015. Preface. Coronaviruses. Methods Mol. Biol. 1282 https://doi.org/10.1007/978-1-4939-2438-7.

Plante, J.A., et al., 2020. Spike mutation D614G alters SARS-CoV-2 fitness and neutralization susceptibility. bioRxiv. https://doi.org/10.1101/2020.09.01.278689.

Selvaraj, Prabhuanand, et al., 2021. SARS-CoV-2 infection induces protective immunity and limits transmission in Syrian hamsters. Life Sci. Alliance. In press.

Yurkovetskiy, L., et al., 2020. SARS-CoV-2 Spike protein variant D614G increases infectivity and retains sensitivity to antibodies that target the receptor binding domain. bioRxiv. https://doi.org/10.1101/2020.07.04.187757.

Zhang, L., Jackson, C.B., Mou, H., Ojha, A., Rangarajan, E.S., Izard, T., Farzan, M., Choe, H., 2020. The D614G mutation in the SARS-CoV-2 spike protein reduces S1 shedding and increases infectivity. bioRxiv. https://doi.org/10.1101/2020.06.12.148726.